

A NEURAL-OPERATOR PRECONDITIONED NEWTON METHOD FOR ACCELERATED NONLINEAR SOLVERS *

YOUNGKYU LEE[†], SHANQING LIU[†], JEROME DARBON[†], AND GEORGE EM
KARNIDAKAIS[†]

Abstract. We propose a novel neural preconditioned Newton (NP-Newton) method for solving parametric nonlinear systems of equations. To overcome the stagnation or instability of Newton iterations caused by unbalanced nonlinearities, we introduce a fixed-point neural operator (FPNO) that learns the direct mapping from the current iterate to the solution by emulating fixed-point iterations. Unlike traditional line-search or trust-region algorithms, the proposed FPNO adaptively employs negative step sizes to effectively mitigate the effects of unbalanced nonlinearities. Through numerical experiments we demonstrate the computational efficiency and robustness of the proposed NP-Newton method across multiple real-world applications, especially for very strong nonlinearities.

Key words. scientific machine learning, nonlinear preconditioning, neural operator, Newton’s method, hybridization

MSC codes. 90C06, 65M55, 65F08, 65F10, 68T07

1. Introduction. The numerical solution of the nonlinear system of equations is required in many engineering applications, i.e., for a given parametric nonlinear function $\mathcal{F}: \mathbb{R}^n \rightarrow \mathbb{R}^n$, we find a vector $u \in \mathbb{R}^n$ such that

$$(1.1) \quad \mathcal{F}(u) = 0.$$

Here $\mathcal{F} = (\mathcal{F}_1, \dots, \mathcal{F}_n)^T$, $\mathcal{F}_i = F_i(u_1, \dots, u_n)$, and $u = (u_1, \dots, u_n)^T$. The Newton’s method is commonly used to solve the nonlinear system of equations (1.1). Suppose $u^{(k)}$ is the current approximate solution: a new approximate solution $u^{(k+1)}$ is computed by

$$u^{(k+1)} = u^{(k)} + \lambda^{(k)} p^{(k)},$$

where the step size $\lambda^{(k)}$ is simply set to 1 or determined by line search algorithms [9], or the update direction $p^{(k)}$ is computed by solving the following linear system

$$(1.2) \quad J^{(k)} p^{(k)} = -\mathcal{F}(u^{(k)}).$$

Here, $J^{(k)} = \mathcal{F}'(u^{(k)})$ is the Jacobian of $\mathcal{F}(u^{(k)})$. For simplicity, we assume that $J^{(k)}$ is nonsingular. When $J^{(k)}$ is singular, the Moore–Penrose inverse [44], the Levenberg–Marquardt method [30, 40], and the arc-length continuation method [22] are commonly used to find the approximated update direction.

When the initial guess is sufficiently close to the solution, the Newton’s method achieves fast, second-order convergence (under appropriate assumptions). However, obtaining such a good initial guess is generally difficult, especially when nonlinear equations have *unbalanced nonlinearities* [26]. Here, unbalanced nonlinearities indicate that the effective step size is dominated by a subset of the total degrees of freedom, which may lead to stagnation in the nonlinear residual curve [5, 6, 10].

*Submitted to the editors November 13, 2025.

Funding: This work was funded by the DARPA-DIAL grant HR00112490484.

[†]Division of Applied Mathematics, Brown University, Providence, RI youngkyu_lee@brown.edu, shanqing_liu@brown.edu, jerome_darbon@brown.edu, george_karniadakis@brown.edu.

Recently, nonlinearly preconditioned Newton methods [6, 7, 10, 23, 39] have attracted attention to address this challenge. The main idea of nonlinear preconditioning is to replace the original nonlinear system $\mathcal{F}(u) = 0$ with an equivalent nonlinear system $\tilde{\mathcal{F}}(u) = 0$. Note that two nonlinear systems are equivalent if they have the same solution. Specifically, $\tilde{\mathcal{F}}$ may take the form of a composite function

$$\tilde{\mathcal{F}}(u) := \mathcal{M}(\mathcal{F}(u)) \text{ or } \mathcal{F}(\mathcal{M}(u)).$$

Here, $\mathcal{M}: \mathbb{R}^n \rightarrow \mathbb{R}^n$ is the preconditioner. ASPIN [6, 39] and RASPEN [10] utilize the additive Schwarz method or restricted additive Schwarz method as the left-preconditioner \mathcal{M} , which gives the nonlinearly preconditioned residual

$$\mathcal{F}_L(u) = \mathcal{M}(\mathcal{F}(u)) = x - \mathcal{M}(x).$$

That is, the left-preconditioning strategy first computes the residual using a fixed-point method and applies the Newton's method to solve $\mathcal{F}_L(u) = 0$. On the other hand, NEPIN [7], nonlinear FETI-DP and BDDC methods [23] utilize the nonlinear elimination technique as the right preconditioner \mathcal{M} , which gives the nonlinearly preconditioned residual

$$\mathcal{F}_R(u) = \mathcal{F}(\mathcal{M}(u)).$$

Hence, the right-preconditioning strategy first applies the right-preconditioner \mathcal{M} using a fixed-point iteration, and then applies the Newton's method to solve $\mathcal{F}_R(u) = 0$. Furthermore, several approaches that design the efficient coarse space for ASPIN and RASPEN [14, 16] and combine with the field-split technique [34] have been proposed.

Recently, operator learning, a subfield of scientific machine learning, offers a powerful alternative to traditional methods for solving nonlinear system of equations. In operator learning, a neural operator (NO) is employed to approximate the solution operator of a given problem by learning the mapping between function spaces, with applications that include resolving a solution from material properties, determining an initial condition from a future state (i.e., solving an inverse problem), and mapping between different state variables [33, 35, 36, 48]. A significant advantage of this framework is that the trained NO can infer the solution for new input function in real-time without costly retraining. However, a notable limitation is the spectral bias of neural networks, which prioritizes learning low-frequency modes. This bias makes it difficult to capture high-frequency modes, making it challenging to obtain machine-accurate solution [45].

On the other hand, the idea of enhancing the convergence of iterative solvers through hybridization with machine learning has recently gained significant attention. Various approaches have been explored in this direction, such as accelerating Krylov subspace methods [21, 38], learning or correcting the Newton directions [12, 20], developing more effective and adaptive preconditioners [11, 15, 25, 31], and leveraging the spectral bias of neural networks to design more efficient coarse-level problems in multilevel solvers [8, 24, 29, 27, 28, 50]. These studies demonstrate that the synergy between numerical algorithms and machine learning is gradually expanding, aiming to achieve faster convergence rates, enhanced robustness, and improved generalization capabilities across diverse problem settings.

In this work, we propose a novel nonlinearly right-preconditioning strategy to enhance the performance of the Newton's method using the pretrained neural operator. The key idea is to mitigate the stagnation arising from unbalanced nonlinearities

in a nonlinear system of equations by leveraging the neural operator. To this end, we introduce a fixed point neural operator (FPNO) that learns the direct mapping from the current iterate to the solution by emulating the fixed-point iteration. By learning the underlying fixed-point map, the FPNO effectively captures the nonlinear relationship between successive Newton iterates, leading to faster and more robust convergence. Enabling the FPNO to use negative step sizes allows the neural preconditioned Newton method to overcome stagnation or instability via negative Newton directions. Furthermore, FPNO can employ many kinds of neural operator architectures such as DeepONets [19, 35, 36], FNOs [32, 33], Transformers [37, 42, 46, 49]. Numerical results confirm that the proposed neural preconditioned Newton method achieves fast convergence and reduced computational time.

The rest of the paper is organized as follows. We first introduce the nonlinearly right-preconditioned Newton method and propose the fixed point neural operator that is used to build the neural preconditioner in Section 2. Section 3 introduces the benchmark problems to demonstrate the capabilities of the proposed neural preconditioned Newton method. The numerical experiments appear in Section 4. Finally, we conclude this paper with a summary in Section 5.

2. A neural preconditioned Newton method. In this section, we first briefly describe the nonlinearly right-preconditioning strategy, which is employed to construct the neural preconditioned Newton method in this paper. Let us recall that we find a vector $u^* \in \mathbb{R}^n$ such that $\mathcal{F}(u^*) = 0$. A nonlinear preconditioner \mathcal{M} of the nonlinear function \mathcal{F} is defined as $\mathcal{M} \approx \mathcal{F}^{-1}$.

The right-preconditioned Newton method applies the Newton’s method to the nonlinearly right-preconditioned residual

$$\tilde{\mathcal{F}}(u) = \mathcal{F}(\mathcal{M}(u)).$$

Starting from the initial guess $u^{(0)}$, the iteration of the right-preconditioned Newton method is defined as

$$\begin{aligned} v^{(k)} &= \mathcal{M}(u^{(k)}), \\ u^{(k+1)} &= v^{(k)} - \lambda^{(k)} (\mathcal{F}'(v^{(k)}))^{-1} \mathcal{F}(v^{(k)}). \end{aligned}$$

Here, the step size $\lambda^{(k)}$ is typically determined using a line search [9], trust-region algorithm [47] or simply set to 1.

On the other hand, in general, it is not easy to obtain such a preconditioner \mathcal{M} explicitly, but such an operator can be defined implicitly as a fixed-point nonlinear iteration, which is given by $u = \mathcal{M}(u)$. Inspired by the fixed-point nonlinear iteration, we construct the nonlinear right-preconditioner \mathcal{M} using a neural operator \mathcal{G} and make the neural operator learn the fixed-point nonlinear iteration. Motivated by the fixed-point nonlinear iteration, we design the nonlinear right-preconditioner \mathcal{M} with a neural operator \mathcal{G} , training \mathcal{G} to emulate the fixed-point nonlinear iteration.

Let N denote the input size of the neural operator. Suppose we have a canonical restriction operator $R: \mathbb{R}^n \rightarrow \mathbb{R}^N$ and a canonical prolongation operator $P: \mathbb{R}^N \rightarrow \mathbb{R}^n$. Then, the neural operator $\mathcal{G}: \mathbb{R}^N \rightarrow \mathbb{R}^N$ is trained to approximate the inverse of the nonlinear function \mathcal{F} such that

$$(2.1) \quad \mathcal{G}(v) \approx (R \circ \mathcal{F}^{-1} \circ P)(v), \quad \forall v \in \mathbb{R}^N.$$

Then, the right-preconditioner $\mathcal{M}: \mathbb{R}^n \rightarrow \mathbb{R}^n$ is naturally defined as

$$\mathcal{M} = P \circ \mathcal{G} \circ R.$$

Without loss of generality, we assume that $n = N$, which enables us to set $\mathcal{M} = \mathcal{G}$.

In order to emulate the fixed-point nonlinear iteration, we propose a novel neural operator called *Fixed Point Neural Operator* (FPNO) given by

$$(2.2) \quad \begin{aligned} r &= \mathcal{F}(u), \quad \tilde{r} = r / \|r\|_2, \\ \eta &= \tanh(\|r\|_2 \mathcal{N}(\tilde{r})), \\ \mathcal{G}(u) &:= u + \eta \cdot \mathcal{G}_B(u). \end{aligned}$$

Here, \mathcal{N} denotes a trainable neural network that takes the normalized residual vector \tilde{r} and produces a scalar output, while \mathcal{G}_B represents a backbone neural operator that takes the vector $u \in \mathbb{R}^N$ as the input and produces a correction vector. When the iterate is converging to the solution, the norm of the residual $\|r\|_2$ is going to 0, which implies the step size $\eta \rightarrow 0$ and $\mathcal{G}(u) = u$. That is, the proposed FPNO learns an approximate inverse of the nonlinear function \mathcal{F} by emulating the fixed-point iteration, enabling it to act as a right-preconditioner for the Newton's method.

Furthermore, since the range of the hyperbolic tangent function is $(-1, 1)$, the predicted step size η can be negative, which allows the FPNO to learn more robust iterations. For example, if the Newton direction computed by (1.2) fails to reduce the residual, the line search or the trust-region algorithm may choose an extremely small step size, such as 10^{-14} , which can lead to stagnation. In contrast, the FPNO can employ a negative step size and thus avoids this problem. A graphical description of the proposed neural preconditioned Newton method using FPNO is shown in Figure 1.

Remark 2.1. The backbone neural operator \mathcal{G}_B is flexible and can be implemented using various neural operator architectures, such as DeepONet [35], FNO [33], or DeepOKAN [1]. When solving parametric PDEs, the structure of \mathcal{G}_B can be further adapted to account for the PDE parameters. Specifically, the PDE parameter can be included as an additional input to \mathcal{G}_B , allowing the operator to learn parameter-dependent solution mappings. In such cases, multi-input neural operators like MIONet [19] are particularly suitable. In this work, we use MIONet as the backbone neural operator to effectively handle parametric PDEs.

Lastly, in order to efficiently train the FPNO, the data generation is important. We first sample an initial guess $u_j^{(0)}$ from a Gaussian random field (GRF) and scale it to the range 10^{-4} – 10^{-2} . Next, we solve $\mathcal{F}(u) = 0$ starting from the initial guess $u_j^{(0)}$ and collect the Newton iteration snapshots

$$\mathcal{D}_j = \left\{ \left(u_j^{(i)}, u_j^* \right) \right\}_{i=0}^{m_j},$$

where m_j denotes the total number of iterations of the Newton method starting from the initial guess $u_j^{(0)}$ and u_j^* is the reference solution. When solving parametric PDEs, the PDE parameter ζ_j is sampled from a given distribution, and the corresponding Newton iteration snapshots are collected as

$$\mathcal{D}_j = \left\{ \left(\zeta_j, u_j^{(i)}, u_j^* \right) \right\}_{i=0}^{m_j}.$$

Note that, in the case of DeepONet variants, we also collect the coordinates x_j cor-

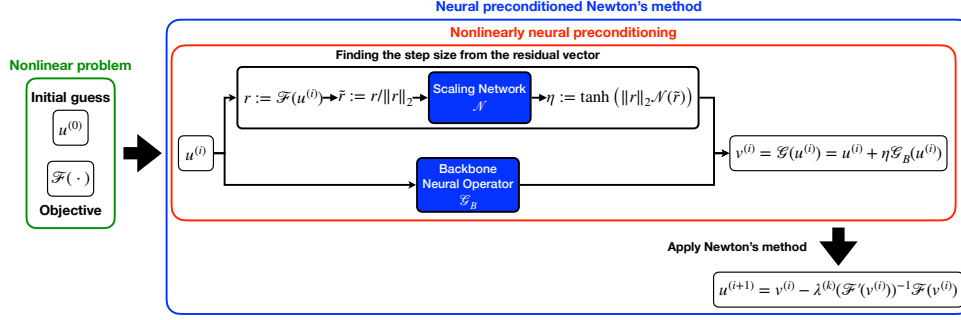


FIG. 1. A schematic of neural preconditioned Newton method using the fixed point neural operator (FPNO) with backbone neural operator \mathcal{G}_B . Starting from the initial guess $u^{(0)}$, the FPNO is first applied to get the smoothed iterate $v^{(i)}$ and the Newton's method is applied to obtain the next iterate $u^{(i+1)}$.

responding to the degrees of freedom. Finally, the training dataset \mathcal{D} is defined as

$$\mathcal{D} := \{\mathcal{D}_j\}_{j=1}^m,$$

where m denotes the total number of random initial guesses. Note that, the total number of training samples is $\sum_{j=1}^m m_j$.

Finally, during the training stage, the FPNO learns the fixed-point nonlinear iteration mapping from the input $u_j^{(i)}$ to the reference solution u_j^* . This implies that when the input is far from u_j^* , the FPNO effectively learns a direct update from the input to the solution, whereas when the input is close to u_j^* , it learns the Newton update direction.

3. Benchmark problems and implementation details. In this section, we present a collection of benchmark problems for demonstrating the performance of the proposed neural preconditioned Newton method.

3.1. Nonlinear Poisson equation. Let $\Omega = (0, 1)^2 \subset \mathbb{R}^2$ and $\Gamma = \{(x, y) \in \partial\Omega | x = 1\}$. The two-dimensional nonlinear Poisson equation is given as

$$(3.1) \quad \begin{cases} -\nabla \cdot (q(u) \nabla u) = f, & \text{in } \Omega, \\ u = 1, & \text{on } \Gamma, \\ \frac{\partial u}{\partial n} = 0, & \text{on } \partial\Omega \setminus \Gamma, \end{cases}$$

where $q(u) = 0.01 + u^2$ and f stands for the forcing term, respectively. We discretized the domain Ω into linear triangular elements with a mesh size of h , denoted as \mathcal{T}_h . Then, solving the equation (3.1) is equivalent to finding $u \in V$ such that

$$(3.2) \quad \mathcal{F}(u) = \int_{\Omega} q(u) \nabla u \nabla v dx - \int_{\Omega} f v dx = 0, \quad \forall v \in V.$$

Here, $V = \{v \in H^1(\Omega) : v|_T \in P^1(T) \quad \forall T \in \mathcal{T}_h, u = 1 \text{ on } \Gamma\}$. Note that $P^1(T)$ is the space of piecewise linear polynomials defined on T . Figure 2 presents an example of the numerical solution of (3.2) computed on 129×129 mesh.

The equation (3.1) is parameterized in terms of the forcing term f . The forcing term f is sampled using Gaussian random field (GRF) with mean $\mathbb{E}[f(x)] = 0.0$ and

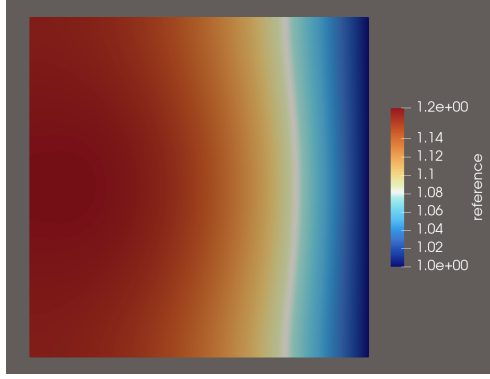


FIG. 2. The numerical solution of nonlinear Poisson equation (3.2) computed on 129×129 mesh, where $q(u) = 0.01 + u^2$ and $f(x, y) = \sin(\pi x) \sin(\pi y)$.

the covariance

$$(3.3) \quad \text{cov}(f(x), f(y)) = \sigma^2 e^{-\frac{\|x-y\|^2}{2\ell^2}} \quad \forall x, y \in \Omega.$$

The parameter σ and ℓ are chosen as $\sigma = 0.1$ and $\ell = 0.1$.

3.2. Hyper elasticity. We next consider the compressible Neo-Hookean model, a popular hyper elasticity model, applied to a square with an oval-shaped hole. Let $\Omega \subset (0, 1)^2 \subset \mathbb{R}^2$ and $\partial\Omega = \Gamma_1 \cup \Gamma_2 \cup \Gamma_3$, where Γ_1 , Γ_2 , and Γ_3 are the bottom boundary, top boundary, and other boundaries, respectively. We discretized the domain Ω into linear quadrilateral elements with a mesh size of h , denoted as \mathcal{T}_h . Then, the minimization problem of the two-dimensional compressible Neo-Hookean model is given as

$$(3.4) \quad \min_{u \in V} \mathcal{L}(u) := \int_{\Omega} \frac{\mu}{2} (I_c - 3) - \mu \ln(J_F) + \frac{\lambda}{2} (J_F - 1)^2 dx,$$

where

$$\begin{cases} V = \{u \in [H^1(\Omega)]^2 : u|_T \in [P^1(T)]^2 \quad \forall T \in \mathcal{T}_h, \\ \quad u = (0, 0) \text{ on } \Gamma_1 \text{ and } u = (0, u_t) \text{ on } \Gamma_2\}, \\ \mu = \frac{E}{2(1+\nu)}, \lambda = \frac{E\nu}{(1+\nu)(1-2\nu)}, \\ F = I + \nabla u, I_c = \text{tr}(F^T F), J_F = \det(F). \end{cases}$$

Note that we set $E = 1.0$ and $\nu = 0.49$ to model rubber-like materials, which withstand large deformations.

The minimization problem (3.4) is solved by finding a solution $u \in V$ that satisfies the optimality condition

$$(3.5) \quad \frac{\partial \mathcal{L}}{\partial u} = \mathcal{F}(u) = 0.$$

Figure 3 shows an example of the computed displacement u and the initial mesh. The problem (3.4) is parameterized in terms of the y -displacement u_t on the top boundary, which is sampled from the uniform distribution $U(0, 2)$.

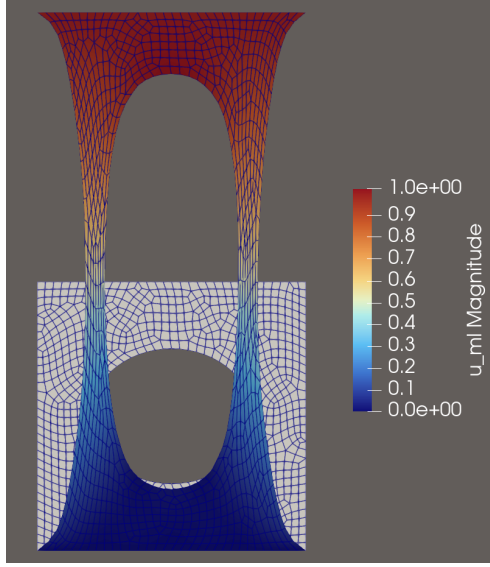


FIG. 3. The computed displacement of hyper elasticity problem (3.4) in $\Omega \subset (0, 1)^2$ when $u_t = 1$ and the maximum mesh size $h = 1/32$. Note that the gray object is the initial mesh.

3.3. Implementation details. We use the FEniCS library [4] to implement the finite element discretization of the benchmark problems and to generate the training samples for the FPNs. To handle parametric PDEs, we adopt the MIONets [19] as the backbone neural operator of the FPNs and refer to the resulting model as the FP-MIONets. The FP-MIONets are implemented using PyTorch [43] and trained using the AdamW optimizer [18], with a batch size of 100, a weight decay of 5×10^{-4} , and a learning rate of 10^{-4} . The training process stops if the average relative L^2 error of the validation samples does not improve for 1,000 consecutive epochs. Note that the relative mean squared error loss function is used for training, which is given as

$$\mathcal{L}_{\text{rel}}(u_\theta, u_{\text{ref}}) = \frac{1}{m} \sum_{i=1}^m \frac{(u_\theta^{(i)} - u_{\text{ref}}^{(i)})^2}{(u_{\text{ref}}^{(i)})^2 + \varepsilon},$$

where $u_\theta = (u_\theta^{(1)}, \dots, u_\theta^{(m)})$ and $u_{\text{ref}} = (u_{\text{ref}}^{(1)}, \dots, u_{\text{ref}}^{(m)})$ are the prediction of the neural network and the reference solution, respectively. Note that the symbol m denotes the batch size, and a small constant $\varepsilon = 10^{-4}$ is added to prevent the loss term from blowing up when $u_{\text{ref}}^{(i)} = 0$. Details about the network architectures, size of datasets, and training times are described in Section A.

The proposed neural preconditioned Newton methods are implemented using PETSc library [3]. The preconditioning of the Newton's method with the FP-MIONet is implemented using the petsc4py interface. Note that the python implementation is not compiled and conducted without hyperparameter tuning, suggesting that the practical performance can be further enhanced. All numerical experiments are conducted using the Oscar supercomputer at Brown University, whose computing node is equipped with an AMD EPYC 9554 64-Core Processor (256GB) and an NVIDIA L40S GPU (48GB).

4. Numerical results. In this section, we present numerical experiments to evaluate the performance of the proposed neural preconditioned Newton method. The Newton method with cubic backtracking line search (Newton-LS) and the Newton method with trust region (Newton-TR) are chosen as the baseline method. We construct the neural preconditioned Newton method combining the pretrained FP-MIONets with Newton-LS and Newton-TR, denoted as NP-Newton-LS and NP-Newton-TR, respectively. All local problems associated with the computation of the Newton direction (1.2) are solved by the MUMPS direct solver [2]. All Newton methods terminate when either of the following criteria is satisfied:

$$\|\mathbf{r}^{(i)}\|_2 \leq 10^{-15} \quad \text{or} \quad \frac{\|\mathbf{r}^{(i)}\|_2}{\|\mathbf{r}^{(0)}\|_2} \leq 10^{-9}.$$

4.1. Nonlinear Poisson equation with various forcing term. First, we solve the nonlinear Poisson equation (3.1) with Newton-LS and NP-Newton-LS. We consider the following three cases of the forcing term f to verify the robustness of the proposed NP-Newton-LS:

- I: $f \equiv 1$.
- II: $f \sim \text{GRF}(\nu, \sigma, \ell)$, where $\nu = 0.0$, $\sigma = 0.1$, and $\ell = 0.1$. Note that the FP-MIONet is trained on this case.
- III: $f \sim \text{GRF}(\nu, \sigma, \ell)$, where $\nu = 0.0$, $\sigma = 1.0$, and $\ell = 0.1$. Unlike the previous case, f can take the high frequency value.

Here, $\text{GRF}(\nu, \sigma, \ell)$ denotes the GRF with mean ν and the covariance defined in (3.3) using σ and ℓ . Furthermore, to demonstrate robustness in resolution and highlight the effectiveness of the proposed NP-Newton-LS particularly on fine meshes, we conduct tests on two meshes \mathcal{T}_{h_1} and \mathcal{T}_{h_2} . Note that $h_1 = 1/32$ and $h_2 = 1/128$, where the FP-MIONet is mainly trained on the coarse mesh \mathcal{T}_{h_1} .

Figure 4 compares the convergence behavior of the Newton-LS method and the proposed NP-Newton-LS method for the nonlinear Poisson equation. For the NP-Newton-LS, the FP-MIONet that is pretrained in the coarse mesh \mathcal{T}_{h_1} is employed as a nonlinear right-preconditioner to enhance the convergence of Newton's method. As shown in the figure, the Newton-LS occasionally suffers from an increase in the residual norm during the Newton iteration, particularly in Case III, where the method eventually diverges. This phenomenon is mainly attributed to the unbalanced nonlinearities of given nonlinear problem, which lead to an unstable search direction in the standard Newton iteration. In contrast, the NP-Newton-LS effectively mitigates this issue, maintaining a monotonic decrease in the residual norm across all cases, demonstrating the stabilizing effect of the proposed neural preconditioning strategy.

Tables 1 and 2 summarize the number of iterations and the computational times for the coarse mesh \mathcal{T}_{h_1} and the fine mesh \mathcal{T}_{h_2} , respectively. In all test cases, the NP-Newton-LS significantly reduces the number of iterations compared to the Newton-LS, achieving substantial computational speed-up. Notably, in Cases I and II, the iteration counts are reduced by more than 50%, and the total computational time decreases accordingly. In Case III, the Newton-LS fails to converge due to the unbalanced nonlinearities, whereas the NP-Newton-LS successfully converges within only a few iterations. These results clearly demonstrate that the neural operator based nonlinear preconditioning improves both the convergence rate and the robustness of Newton's method.

4.2. Hyper elasticity problem with small and large deformation. Next, we solve the hyper elasticity problem (3.4) with Newton-LS, Newton-TR, NP-Newton-

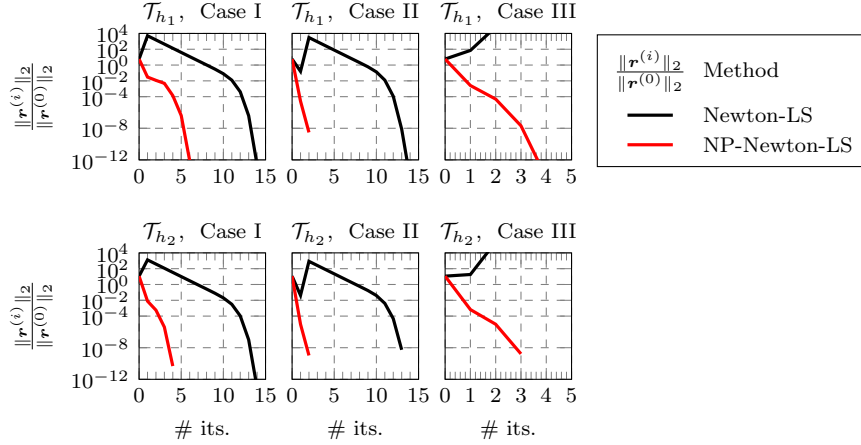


FIG. 4. The convergence of the Newton's method for the nonlinear Poisson equation. The first row shows the results for the coarse mesh, and the second row shows the results for the fine mesh. In Case III, the Newton-LS method diverges, and the iteration is terminated when the relative residual norm exceeds 10^4 .

TABLE 1

The number of iterations and the computational time in seconds (s) required by the Newton-LS and NP-Newton-LS for different cases in the coarse mesh \mathcal{T}_{h1} . In Case III, since the relative residual norm of Newton-LS exceeds 10^4 , the Newton iteration is terminated and noted as divergent.

Case	Method	# iterations	Time (s)	Speed-up
I	Newton-LS	14	0.0710	-
	NP-Newton-LS	6	0.0671	5.81%
II	Newton-LS	14	0.0795	-
	NP-Newton-LS	2	0.0336	136.60%
III	Newton-LS	diverge	-	-
	NP-Newton-LS	4	0.0455	∞

TABLE 2

The number of iterations and the computational time in seconds (s) required by the Newton-LS and NP-Newton-LS for different cases in the fine mesh \mathcal{T}_{h2} . Similar to the coarse mesh, in Case III, since the relative residual norm of Newton-LS exceeds 10^4 , the Newton iteration is terminated and noted as divergent.

Case	Method	# iterations	Time (s)	Speed-up
I	Newton-LS	14	0.5435	-
	NP-Newton-LS	4	0.2768	96.35%
II	Newton-LS	13	0.5030	-
	NP-Newton-LS	2	0.1575	219.37%
III	Newton-LS	diverge	-	-
	NP-Newton-LS	3	0.1985	∞

LS, and NP-Newton-TR. In order to highlight the performance of the proposed NP-Newton-LS and NP-Newton-TR, we consider the following two cases of the top displacement corresponding to small and large deformations:

- I: $u_t = 0.1$. In this case, the computed displacement is quite similar with the displacement computed from the linear elasticity model.
- II: $u_t = 1$. In this case, the Newton-LS method fails to converge without additional techniques. To address this issue, we employ the incremental loading technique [41], a common approach for mitigating unbalanced nonlinearities, with a loading step size of $\delta u_t = 0.1$. Specifically, the total loading is applied gradually in several increments rather than in a single step, which allows the Newton's method to trace the equilibrium path more stably. At each increment, the solution obtained from the previous step serves as an initial guess for the next, thereby improving convergence and preventing divergence due to large deformation. The resulting method is referred to as IC-Newton-LS.

Moreover, we also consider the coarse mesh \mathcal{T}_{h_1} and the fine mesh \mathcal{T}_{h_2} to further investigate the robustness of the proposed methods with respect to mesh resolution. The corresponding numbers of degrees of freedom for \mathcal{T}_{h_1} and \mathcal{T}_{h_2} are summarized in Table 6.

Figure 5 provides the convergence histories for the relative residual norm on two different meshes \mathcal{T}_{h_1} and \mathcal{T}_{h_2} . The performance of the proposed neural preconditioned Newton methods (NP-Newton-LS and NP-Newton-TR) is compared against the Newton's methods (Newton-LS and Newton-TR) and the incremental loading method (IC-Newton-LS). Similar to the case of the nonlinear Poisson equation, the FP-MIONet used to construct the neural preconditioner is pretrained in the coarse mesh \mathcal{T}_{h_1} . In the simpler Case I, all methods successfully converge. The proposed NP-Newton-LS and NP-Newton-TR exhibit the fastest convergence in terms of iteration count, requiring only 3 iterations on both meshes. Note that the convergence behaviors of NP-Newton-LS and NP-Newton-TR are nearly identical, and their plots overlap. The effectiveness and robustness of the proposed framework are most evident in the more challenging Case II. Since the Newton-LS method fails to converge, the Newton-TR method is used as the baseline when the incremental loading technique is not applied. It requires over 100 and 200 iterations for the \mathcal{T}_{h_1} and \mathcal{T}_{h_2} meshes, respectively. By employing the incremental loading technique, the IC-Newton-LS method significantly outperforms the standard Newton-TR method in terms of stability and convergence, with convergence attained in roughly 40 iterations. On the other hand, the proposed NP-Newton-TR demonstrates exceptional performance. It converges robustly in fewer than 10 iterations on both coarse and fine meshes.

Tables 3 and 4 summarize the number of iterations and the computational times for both coarse and fine meshes. In Case I, although the NP-Newton-LS reduces the number of iterations by approximately half compared with the Newton-LS, the actual computational speed-up is negative for both coarse and fine meshes. However, the degradation is noticeably smaller on the fine mesh than on the coarse mesh. On the other hand, the NP-Newton-TR significantly reduces the number of iterations compared with the Newton-TR, achieving actual computational speed-ups of 71.03% and 246.47%, respectively. In Case I where the deformation is minimal, the Newton's method does not suffer from unbalanced nonlinearity. Therefore, since the cost of preconditioning using a neural operator is higher, we can conclude that no practical speedup can be achieved.

However, the situation changes drastically under the large deformation. In Case II, due to the unbalanced nonlinearities, the Newton-LS fails to converge entirely,

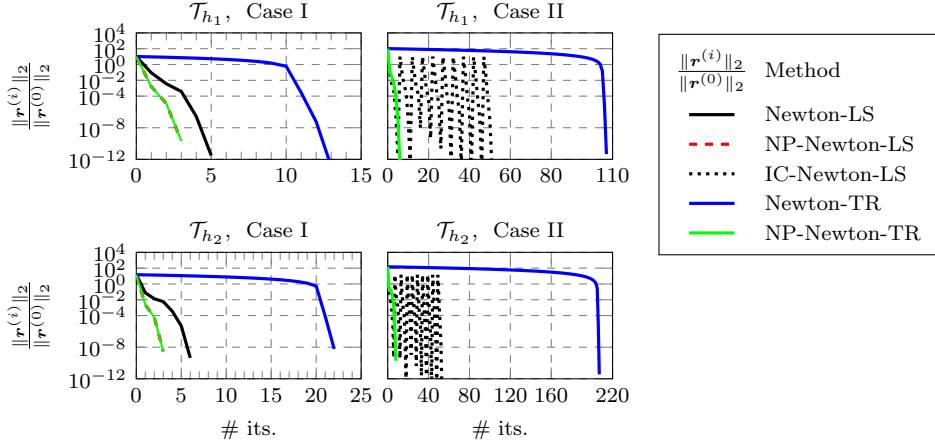


FIG. 5. Convergence of Newton's method for the hyper elasticity problem. Since the IC-Newton-LS uses the incremental loading technique, the history of the relative residual norm is concatenated. In Case I, the convergence behaviors of NP-Newton-LS and NP-Newton-TR are almost identical, so their plots overlap.

while the Newton-TR requires a substantially large number of iterations to reach a solution. A well-known approach to mitigate this issue is the incremental loading technique, denoted as IC-Newton-LS. As reported in both tables, IC-Newton-LS effectively stabilizes the solution process, significantly reducing the total number of iterations and achieving actual computational speed-ups of 143.04% and 331.33% on the coarse and fine meshes, respectively, compared with the Newton-TR. In contrast, our proposed NP-Newton-TR exhibits remarkable efficiency and robustness: it converges to the solution in only 6 iterations on the coarse mesh and 8 iterations on the fine mesh. This corresponds to extraordinary actual computational speed-ups of 597.89% and 1130.46%, respectively, demonstrating the superiority of the NP-Newton-TR in handling hyper elasticity problem with large deformation. These results highlight that the combination of the proposed FPNO-based neural preconditioning and the trust-region algorithm provides a highly robust and efficient solver for challenging nonlinear problems.

5. Summary. We proposed a novel nonlinearly right-preconditioning framework to accelerate Newton's method using a pretrained neural operator. In particular, we introduced the fixed-point neural operator (FPNO), which learns the direct mapping from the current Newton iterate to the reference solution by emulating the fixed-point iteration of a given nonlinear function. In order to address unbalanced nonlinearities, the proposed FPNO adaptively allows the negative step sizes based on the residual direction. Moreover, FPNO is compatible with various neural operator architectures such as DeepONet, FNO, and Transolver; in this work, MIONet was employed for implementation to handle the parametric nonlinear PDEs. The performance of the proposed neural preconditioned Newton method was evaluated through benchmark problems, showing its capability to enhance convergence.

The presented framework can be extended in several promising directions. To handle large-scale domains, the domain decomposition method based nonlinear preconditioners such as ASPIN [6], RASPEN [10], NEPIN [7], and nonlinear FETI-DP and BDDC methods [23] are widely used as state-of-the-art preconditioners for the

TABLE 3

The number of iterations and the computational time in seconds (s) required by the Newton-LS, Newton-TR, IC-Newton-LS, NP-Newton-LS, and NP-Newton-LS for different cases in the coarse mesh \mathcal{T}_{h_1} .

Case	Method	# iterations	Time (s)	Speed-up
I	Newton-LS	5	0.0596	-
	NP-Newton-LS	3	0.0901	-33.85%
	Newton-TR	13	0.1529	-
	NP-Newton-TR	3	0.0894	71.03%
II	Newton-TR	107	1.2541	-
	IC-Newton-LS	42	0.5160	143.04%
	NP-Newton-TR	6	0.1797	597.89%

TABLE 4

The number of iterations and the computational time in seconds (s) required by the Newton-LS, Newton-TR, IC-Newton-LS, NP-Newton-LS, and NP-Newton-LS for different cases in the fine mesh \mathcal{T}_{h_2} .

Case	Method	# iterations	Time (s)	Speed-up
I	Newton-LS	6	0.2114	-
	NP-Newton-LS	3	0.2258	-6.38%
	Newton-TR	22	0.7553	-
	NP-Newton-TR	3	0.2180	246.47%
II	Newton-TR	207	6.9841	-
	IC-Newton-LS	44	1.6192	331.33%
	NP-Newton-TR	8	0.5676	1130.46%

Newton’s method. These methods often rely on a coarse-level correction to further accelerate convergence; however, constructing such a structure, e.g., via the full approximation scheme, is often nontrivial [14, 16]. This challenge could be addressed by employing the proposed neural preconditioning framework to construct efficient two-level nonlinear solvers, potentially combining data-driven learning with multi-level strategies.

Appendix A. Details of training procedure of FP-MIONets. In this section, we provide details on the network architectures of the neural operators and their training strategies for all problems discussed in Section 3. We employ the squeeze-and-excitation (SE) operation [17] with a softmax activation function instead of the sigmoid activation function, and integrate it with a residual neural network (ResNet) [13] composed of fully connected layers, denoted as SE-ResNet. Specifically, each layer of the SE-ResNet consists of a fully connected layer followed by a skip connection and an SE operation. Note that we employ the Gaussian error linear unit (GELU) as the activation function in all networks. To predict vector-valued functions, the branch

TABLE 5

The summary of FP-MIONets' architectures. Here, NP and HE denote the nonlinear Poisson and the hyper elasticity, respectively. The symbol S , B , B_f and T represent the scaling, branch, feature-branch and trunk networks in FP-MIONets, respectively. The feature-branch network is introduced to handle physical parameters and corresponds to the second branch network in the MIONet architecture [19]. For the NP, the source term f is used as input, whereas for the HE, the y -component of the displacement is utilized. A fully connected ResNet is employed with the GELU activation function, and a squeeze-and-excitation (SE) block is incorporated to further enhance network performance. The symbol $[\cdot]$ indicates the width for the neural network.

Problem	Subnetworks	Layers	Activation
NP	S	SE-ResNet[1089, 512, 512, 1]	GELU
	B	SE-ResNet[1089, 512, 512, 512, 256]	
	B_f	SE-ResNet[1089, 512, 512, 512, 256]	
	T	ResNet[2, 512, 512, 512, 256]	
HE	S	SE-ResNet[1029, 512, 512, 1]	GELU
	B	SE-ResNet[1029, 512, 512, 512, 512]	
	B_f	SE-ResNet[1, 512, 512, 512, 256]	
	T	ResNet[2, 512, 512, 512, 256]	

TABLE 6

Summary of the number of degrees of freedom associated with meshes for problems in Section 3. Here, NP and HE denote the nonlinear Poisson and the hyper elasticity, respectively. For the NP problem, the unit square domain is discretized using triangular elements, whereas for the HE problem, an unstructured mesh of quadrilateral elements is used to discretize a unit square containing an elliptical hole at the center with a major axis of 0.6 and a minor axis of 0.5.

Problem	\mathcal{T}_{h_1}	\mathcal{T}_{h_2}
NP	1,089	16,641
HE	1,029	3,932

network of the FP-MIONet generates additional coefficients equal to the dimension of the vector, and each component of the vector-valued function is obtained by taking the inner product of these coefficients with the output of the trunk network. The detailed architectures of the FP-MIONets are summarized in Table 5.

Regarding the training datasets, we first summarize the discretized meshes used in the finite element method in Table 6. For each problem, the mesh \mathcal{T}_{h_1} is employed to generate the training datasets for the FP-MIONets. Table 7 provides the training times required for all FP-MIONets, along with the number of samples used in each dataset. Note that the relative L^2 errors on the validation sets are 0.6% and 0.1% for the nonlinear Poisson equation and the hyper elasticity problem, respectively, demonstrating the high accuracy of the trained FP-MIONets.

REFERENCES

- [1] D. W. ABUEIDDA, P. PANTIDIS, AND M. E. MOBASHER, *DeepOKAN: Deep operator network based on kolmogorov arnold networks for mechanics problems*, Computer Methods in Ap-

TABLE 7

Summary of the number of initial guesses (N_g), generated training/validation samples (N_{st}/N_{sv}), the number of epochs, and training time in hours (h) for all problems. Here, NP and HE denote the nonlinear Poisson and the hyper elasticity, respectively.

Problem	N_g	N_{st}/N_{sv}	Epochs	Time (h)
NP	3,150	10,658/1,185	1,921	0.62
HE	2,000	46,257/5,140	3,293	4.12

- plied Mechanics and Engineering, 436 (2025), p. 117699.
- [2] P. R. AMESTOY, I. S. DUFF, J.-Y. L'EXCELLENT, AND J. KOSTER, *A fully asynchronous multi-frontal solver using distributed dynamic scheduling*, SIAM Journal on Matrix Analysis and Applications, 23 (2001), pp. 15–41.
 - [3] S. BALAY, S. ABHYANKAR, M. ADAMS, J. BROWN, P. BRUNE, K. BUSCHELMAN, L. DALCIN, A. DENER, V. ELKHOUT, W. GROPP, ET AL., *Petsc users manual*, tech. report, Argonne National Laboratory, 2019.
 - [4] I. A. BARATTA, J. P. DEAN, J. S. DOKKEN, M. HABERA, J. S. HALE, C. N. RICHARDSON, M. E. ROGNES, M. W. SCROGGS, N. SIME, AND G. N. WELLS, *DOLFINx: the next generation FEniCS problem solving environment*. preprint, 2023, <https://doi.org/10.5281/zenodo.10447666>.
 - [5] X.-C. CAI, W. D. GROPP, D. E. KEYES, R. G. MELVIN, AND D. P. YOUNG, *Parallel Newton–Krylov–Schwarz algorithms for the transonic full potential equation*, SIAM Journal on Scientific Computing, 19 (1998), pp. 246–265.
 - [6] X.-C. CAI AND D. E. KEYES, *Nonlinearly preconditioned inexact Newton algorithms*, SIAM Journal on Scientific Computing, 24 (2002), pp. 183–200.
 - [7] X.-C. CAI AND X. LI, *Inexact Newton methods with restricted additive Schwarz based nonlinear elimination for problems with high local nonlinearity*, SIAM Journal on Scientific Computing, 33 (2011), pp. 746–762.
 - [8] C. CUI, K. JIANG, Y. LIU, AND S. SHU, *Fourier neural solver for large sparse linear algebraic systems*, Mathematics, 10 (2022), p. 4014.
 - [9] J. E. DENNIS JR AND R. B. SCHNABEL, *Numerical methods for unconstrained optimization and nonlinear equations*, SIAM, Philadelphia, 1996.
 - [10] V. DOLEAN, M. J. GANDER, W. KHERIJI, F. KWOK, AND R. MASSON, *Nonlinear preconditioning: How to use a nonlinear Schwarz method to precondition Newton's method*, SIAM Journal on Scientific Computing, 38 (2016), pp. A3357–A3380.
 - [11] M. GOTZ AND H. ANZT, *Machine learning-aided numerical linear algebra: Convolutional neural networks for the efficient preconditioner generation*, in 2018 IEEE/ACM 9th Workshop on Latest Advances in Scalable Algorithms for Large-Scale Systems (scalA), IEEE Computer Society, 2018, pp. 49–56.
 - [12] W. HAO, X. LIU, AND Y. YANG, *Newton informed neural operator for solving nonlinear partial differential equations*, in Advances in Neural Information Processing Systems, A. Globerson, L. Mackey, D. Belgrave, A. Fan, U. Paquet, J. Tomczak, and C. Zhang, eds., vol. 37, Curran Associates, Inc., 2024, pp. 120832–120860.
 - [13] K. HE, X. ZHANG, S. REN, AND J. SUN, *Deep residual learning for image recognition*, in 2016 IEEE Conference on Computer Vision and Pattern Recognition (CVPR), 2016, pp. 770–778.
 - [14] A. HEINLEIN, A. KLAUWONN, AND M. LANSER, *Adaptive nonlinear domain decomposition methods with an application to the p-Laplacian*, SIAM Journal on Scientific Computing, 45 (2022), pp. S152–S172.
 - [15] A. HEINLEIN, A. KLAUWONN, M. LANSER, AND J. WEBER, *Combining machine learning and domain decomposition methods for the solution of partial differential equations—a review*, GAMM-Mitteilungen, 44 (2021), p. e202100001.
 - [16] A. HEINLEIN AND M. LANSER, *Additive and hybrid nonlinear two-level Schwarz methods and energy minimizing coarse spaces for unstructured grids*, SIAM Journal on Scientific Computing, 42 (2020), pp. A2461–A2488.
 - [17] J. HU, L. SHEN, AND G. SUN, *Squeeze-and-Excitation networks*, in 2018 IEEE/CVF Conference on Computer Vision and Pattern Recognition, 2018, pp. 7132–7141.
 - [18] L. ILYA AND H. FRANK, *Decoupled weight decay regularization international conference on learning representations*, in International Conference on Learning Representations, 2019.

- [19] P. JIN, S. MENG, AND L. LU, *MIONet: Learning multiple-input operators via tensor product*, SIAM Journal on Scientific Computing, 44 (2022), pp. A3490–A3514.
- [20] T. JIN, G. MAIERHOFER, K. SCHRATZ, AND Y. XIANG, *A fast neural hybrid Newton solver adapted to implicit methods for nonlinear dynamics*, Journal of Computational Physics, 529 (2025), p. 113869.
- [21] A. KANEDA, O. AKAR, J. CHEN, V. A. T. KALA, D. HYDE, AND J. TERAN, *A deep conjugate direction method for iteratively solving linear systems*, in Proceedings of the 40th International Conference on Machine Learning, A. Krause, E. Brunskill, K. Cho, B. Engelhardt, S. Sabato, and J. Scarlett, eds., vol. 202 of Proceedings of Machine Learning Research, PMLR, 23–29 Jul 2023, pp. 15720–15736.
- [22] H. B. KELLER, *Numerical solution of bifurcation and nonlinear eigenvalue problems.*, Applications of Bifurcation Theory., (1977).
- [23] A. KLAWONN, M. LANSER, O. RHEINBACH, AND M. URAN, *Nonlinear FETI-DP and BDDC methods: a unified framework and parallel results*, SIAM Journal on Scientific Computing, 39 (2017), pp. C417–C451.
- [24] A. KOPANIČÁKOVÁ AND G. E. KARNIADAKIS, *DeepONet based preconditioning strategies for solving parametric linear systems of equations*, SIAM Journal on Scientific Computing, 47 (2025), pp. C151–C181.
- [25] A. KOPANIČÁKOVÁ, Y. LEE, AND G. E. KARNIADAKIS, *Leveraging operator learning to accelerate convergence of the preconditioned conjugate gradient method*, Machine Learning for Computational Science and Engineering, 1 (2025), p. 39.
- [26] P. J. LANZKRON, D. J. ROSE, AND J. T. WILKES, *An analysis of approximate nonlinear elimination*, SIAM Journal on Scientific Computing, 17 (1996), pp. 538–559.
- [27] Y. LEE, S. LIU, J. DARBON, AND G. E. KARNIADAKIS, *Automatic discovery of optimal meta-solvers via multi-objective optimization*, arXiv preprint arXiv:2412.00063, (2024).
- [28] Y. LEE, S. LIU, J. DARBON, AND G. E. KARNIADAKIS, *Automatic discovery of optimal meta-solvers for time-dependent nonlinear pdes*, arXiv preprint arXiv:2507.00278, (2025).
- [29] Y. LEE, S. LIU, Z. ZOU, A. KAHANA, E. TURKEL, R. RANADE, J. PATHAK, AND G. E. KARNIADAKIS, *Fast meta-solvers for 3D complex-shape scatterers using neural operators trained on a non-scattering problem*, Computer Methods in Applied Mechanics and Engineering, 446 (2025), p. 118231.
- [30] K. LEVENBERG, *A method for the solution of certain non-linear problems in least squares*, Quarterly of Applied Mathematics, 2 (1944), pp. 164–168.
- [31] Y. LI, P. Y. CHEN, T. DU, AND W. MATUSIK, *Learning preconditioners for conjugate gradient PDE solvers*, in Proceedings of the 40th International Conference on Machine Learning, A. Krause, E. Brunskill, K. Cho, B. Engelhardt, S. Sabato, and J. Scarlett, eds., vol. 202 of Proceedings of Machine Learning Research, PMLR, 23–29 Jul 2023, pp. 19425–19439.
- [32] Z. LI, D. Z. HUANG, B. LIU, AND A. ANANDKUMAR, *Fourier neural operator with learned deformations for pdes on general geometries*, Journal of Machine Learning Research, 24 (2023), pp. 1–26.
- [33] Z. LI, N. B. KOVACHKI, K. AZIZZADENESHELI, B. LIU, K. BHATTACHARYA, A. STUART, AND A. ANANDKUMAR, *Fourier neural operator for parametric partial differential equations*, in International Conference on Learning Representations, 2021.
- [34] L. LIU AND D. E. KEYES, *Field-split preconditioned inexact Newton algorithms*, SIAM Journal on Scientific Computing, 37 (2015), pp. A1388–A1409.
- [35] L. LU, P. JIN, G. PANG, Z. ZHANG, AND G. E. KARNIADAKIS, *Learning nonlinear operators via DeepONet based on the universal approximation theorem of operators*, Nature machine intelligence, 3 (2021), pp. 218–229.
- [36] L. LU, X. MENG, S. CAI, Z. MAO, S. GOSWAMI, Z. ZHANG, AND G. E. KARNIADAKIS, *A comprehensive and fair comparison of two neural operators (with practical extensions) based on fair data*, Computer Methods in Applied Mechanics and Engineering, 393 (2022), p. 114778.
- [37] H. LUO, H. WU, H. ZHOU, L. XING, Y. DI, J. WANG, AND M. LONG, *Transolver++: An accurate neural solver for pdes on million-scale geometries*, in International Conference on Machine Learning, 2025.
- [38] J. LUO, J. WANG, H. WANG, Z. GENG, H. CHEN, Y. KUANG, ET AL., *Neural Krylov iteration for accelerating linear system solving*, Advances in Neural Information Processing Systems, 37 (2024), pp. 128636–128667.
- [39] L. MARCINKOWSKI AND X.-C. CAI, *Parallel performance of some two-level ASPIN algorithms*, in Domain Decomposition Methods in Science and Engineering, Springer, New York, 2005, pp. 639–646.
- [40] D. W. MARQUARDT, *An algorithm for least-squares estimation of nonlinear parameters*, Journal

- of the Society for Industrial and Applied Mathematics, 11 (1963), pp. 431–441.
- [41] R. OGDEN, *Non-linear Elastic Deformations*, Ellis Horwood series in mathematics and its applications, E. Horwood, New York, 1984.
 - [42] O. OVADIA, A. KAHANA, P. STINIS, E. TURKEL, D. GIVOLI, AND G. E. KARNIADAKIS, *Vito: Vision transformer-operator*, Computer Methods in Applied Mechanics and Engineering, 428 (2024), p. 117109.
 - [43] A. PASZKE, S. GROSS, F. MASSA, A. LERER, J. BRADBURY, G. CHANAN, T. KILLEEN, Z. LIN, N. GIMELSHEIN, L. ANTIGA, A. DESMAISON, A. KOPF, E. YANG, Z. DeVITO, M. RAISON, A. TEJANI, S. CHILAMKURTHY, B. STEINER, L. FANG, J. BAI, AND S. CHINTALA, *Pytorch: An imperative style, high-performance deep learning library*, in Advances in Neural Information Processing Systems, vol. 32, Curran Associates, Inc., 2019.
 - [44] R. PENROSE, *A generalized inverse for matrices*, in Mathematical Proceedings of the Cambridge Philosophical Society, vol. 51, Cambridge University Press, 1955, pp. 406–413.
 - [45] N. RAHAMAN, A. BARATIN, D. ARPIT, F. DRAXLER, M. LIN, F. HAMPRECHT, Y. BENGIO, AND A. COURVILLE, *On the spectral bias of neural networks*, in International Conference on Machine Learning, PMLR, 2019, pp. 5301–5310.
 - [46] B. SHIH, A. PEYVAN, Z. ZHANG, AND G. E. KARNIADAKIS, *Transformers as neural operators for solutions of differential equations with finite regularity*, Computer Methods in Applied Mechanics and Engineering, 434 (2025), p. 117560.
 - [47] D. C. SORENSEN, *Newton's method with a model trust region modification*, SIAM Journal on Numerical Analysis, 19 (1982), pp. 409–426.
 - [48] S. WANG, H. WANG, AND P. PERDIKARIS, *Learning the solution operator of parametric partial differential equations with physics-informed DeepONets*, Science advances, 7 (2021), p. eabi8605.
 - [49] H. WU, H. LUO, H. WANG, J. WANG, AND M. LONG, *Transolver: A fast transformer solver for PDEs on general geometries*, in International Conference on Machine Learning, 2024.
 - [50] E. ZHANG, A. KAHANA, A. KOPANIČÁKOVÁ, E. TURKEL, R. RANADE, J. PATHAK, AND G. E. KARNIADAKIS, *Blending neural operators and relaxation methods in PDE numerical solvers*, Nature Machine Intelligence, 6 (2024), pp. 1303–1313.